



Universiteit
Leiden
The Netherlands

TNFalpha-signaling in drug-induced liver injury

Fredriksson, L.E.

Citation

Fredriksson, L. E. (2012, December 6). *TNFalpha-signaling in drug-induced liver injury*. Retrieved from <https://hdl.handle.net/1887/20257>

Version: Corrected Publisher's Version

License: [Licence agreement concerning inclusion of doctoral thesis in the Institutional Repository of the University of Leiden](#)

Downloaded from: <https://hdl.handle.net/1887/20257>

Note: To cite this publication please use the final published version (if applicable).

Cover Page



Universiteit Leiden

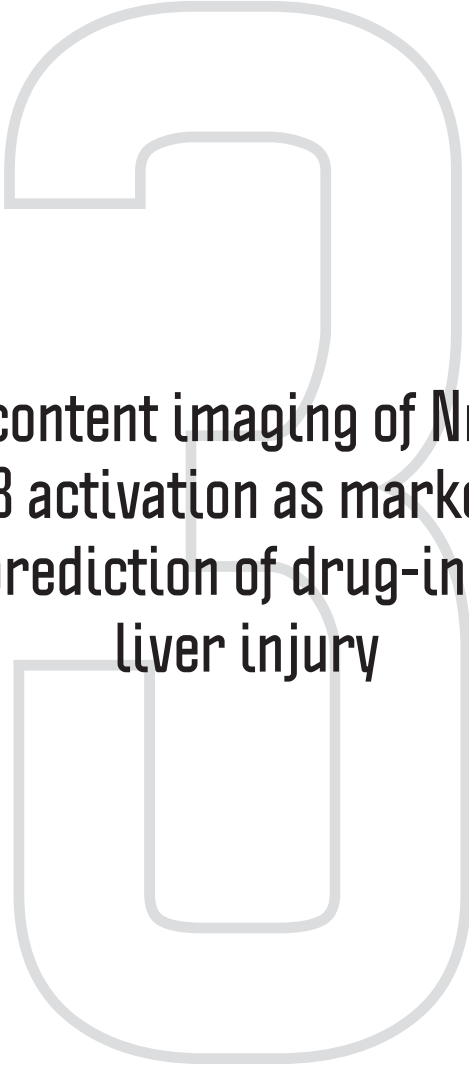


The handle <http://hdl.handle.net/1887/20257> holds various files of this Leiden University dissertation.

Author: Fredriksson, Lisa Emilia

Title: TNFalpha-signaling in drug-induced liver injury

Issue Date: 2012-12-06



**High content imaging of Nrf2 and
NF- κ B activation as markers for
the prediction of drug-induced
liver injury**

Lisa Fredriksson*, Bram Herpers*, Zi Di, Giel Hendriks,
Harry Vrieling, Hans de Bont and Bob van de Water

Submitted to Journal of Hepatology

ABSTRACT

Drug-induced liver injury (DILI) is an important clinical problem, yet predicting human DILI for novel candidate drugs remains difficult. Current models indicate that in many cases DILI is linked to reactive metabolite formation and involves activation of innate immune responses. Here we systematically evaluated the combined application of high content live cell imaging-based analysis of 1) Nrf2 activation as a measure for reactive metabolite stress; 2) perturbations of the normal NF- κ B activation mediated by TNF α ; and 3) synergistic induction of apoptosis by DILI compounds and TNF α . Fifteen drugs associated with DILI were evaluated. Most DILI compounds induced Nrf2 stabilization-dependent activation of the downstream target SRXN1 (11 out of 15). Various DILI compounds diminished the TNF α -induced activation of NF- κ B (6 out of 15), which strongly correlated to the strength of Nrf2 activation. In particular for those compounds that show strong Nrf2 activation and perturbation of NF- κ B signaling, a significant drug-cytokine synergy for apoptosis was observed, which included carbamazepine, diclofenac and ketoconazole, and to a lesser extent clozapine, nefazodone and amiodarone. Together, our data support that mechanism-based high content imaging strategies involving combined analyses of cellular stress responses contribute to DILI hazard identification.

3

Reporters for drug-induced liver injury

INTRODUCTION

Adverse drug reactions are difficult to predict because of a lack in the understanding of the underlying mechanisms (1). Evidence points at the formation of chemically reactive metabolites being one of the initial causes of drug-induced liver injury (DILI) (1, 2), leading to oxidative stress and mitochondrial dysfunction (3). In addition, DILI involves an immune component (4) largely involving the innate immune system with the liver Kupffer cells as critical players (5-8). Activated immune cells release pro-inflammatory cytokines (9) which act on the hepatocytes undergoing reactive metabolite stress. This combination of toxicant and cytokine-induced stress signals may activate a pro-apoptotic response. Indeed, in mouse models non-hepatotoxic drugs (with DILI association in humans) can become hepatotoxic by co-treatment with lipopolysaccharide (LPS) which is dependent on the pro-inflammatory cytokine TNF α (10, 11). This critical role of TNF α in adverse drug-cytokine synergy can be reconstituted in an *in vitro* model by co-exposing liver epithelial cells to drugs linked to DILI in combination with TNF α (12, 13).

Reactive drug metabolite-mediated intracellular perturbations of the cellular redox potential are counterbalanced by the anti-oxidant response under control of the transcription factor Nrf2 (14, 15). Under low oxidative stress conditions Nrf2 is degraded by the proteasome, due to ubiquitination by its inhibitory protein Keap1 (or INrf2) (14). During toxic stress the soft electrophilic reactive metabolites and/or increased levels of reactive oxygen species (ROS) target the cysteine residues in Keap1 (16, 17), allowing Nrf2 to evade the Keap1-mediated repression, and accumulates in the nucleus to activate a diversity of cytoprotective antioxidant target genes (18). Nrf2 is an essential transcription factor for defense against DILI (18), e.g. for the detoxification of acetaminophen (APAP) (19, 20). Interestingly, activation of Nrf2 is also influenced by the p53-p21 axis, autophagy, HSP90 and NF- κ B signaling (21). This indicates that oxidative stress signaling, apoptosis regulation and immune signaling are tightly linked biological programs to accurately control the cell fate decision after toxicant exposure.

TNF α binding to its receptor leads to activation of the tri-partite inhibitor of kappa-B kinase (IKK-) complex (IKK α , IKK β and NEMO). This kinase complex phosphorylates the inhibitor of kappa B (I κ B α), leading to rapid ubiquitination and degradation of this inhibitor directly followed by the release of NF- κ B and nuclear translocation to activate its target genes. A primary early transcriptional target of NF- κ B is I κ B α (NFKBIA), which recruits NF- κ B back into the cytoplasm (resting state), creating an autoregulatory negative feedback loop (22). Hence, NF- κ B activation follows an oscillating nuclear translocation pattern, dependent on the persistence of the cytokine signal and intracellular responses (23). Its periodicity is influenced by redox regulation and dictates the outcome of the genetic response (24). Importantly, we recently established that the hepatotoxicant diclofenac interferes with the NF- κ B oscillatory response in association with a synergy between diclofenac and TNF α to induce apoptosis in liver cells (13). Whether this holds true for other DILI compounds is investigated here.

We established a high content imaging-based strategy using HepG2 cells as

a model to quantitatively follow the onset of apoptosis, Nrf2-dependent activation of Sulfiredoxin (Srxn1) expression, and nuclear oscillation of NF- κ B. These assays were used for concentration- and time-course experiments with a panel of fifteen drugs associated to human DILI: acetaminophen (APAP), 3'-hydroxyacetanilide (AMAP), amiodarone (AMI), carbamazepine (CBZ), clozapine (CLZ), diclofenac (DCF), isoniazid (INH), ketoconazole (KTZ), methotrexate (MTX), nefazodone (NFZ), naproxen (NPX), nitrofurantoin (NTF), ofloxacin (OFX), simvastatin (SN) and troglitazone (TGZ). We studied their effect on cell stress in relation to co-exposure with TNF α . Our results indicate that a strong correlation between Nrf2 activation and inhibition of TNF α -induced NF- κ B nuclear translocation responses. When both of these response pathways are affected, TNF α and DILI compounds synergize to enhance the onset of cell killing.

MATERIALS AND METHODS

Reagents

All drugs were acquired from Sigma-Aldrich and freshly dissolved in DMSO, except for menadione and naproxen (in PBS). Human TNF α was purchased from R&D systems and stored as 10 μ g/mL in 0.1% BSA in PBS aliquots.

Cell culture

Human hepatoma HepG2 cells were acquired from ATCC (clone HB8065) and maintained and exposed to drugs in DMEM high glucose supplemented with 10% (v/v) FBS, 25 U/mL penicillin and 25 μ g/mL streptomycin. The cells were used between passage 5 and 20. For live cell imaging, the cells were seeded in Greiner black μ -clear 96-well plates, at 20,000 cells per well.

Generation of GFP-tagged cell lines

HepG2 cells stably expressing human GFP-p65 as in (13). Mouse Sulfiredoxin (Srxn1) was tagged with GFP at the C-terminus using BAC recombineering (25) and stably introduced into HepG2 cells by transfection and 500 μ g/ml G-418 selection.

RNA interference

siRNAs against human NFE2L2 and KEAP1 were acquired from Dharmacon (ThermoFisher Scientific) as siGENOME SMARTpool reagents, as well as in the form of four individual siRNAs. HepG2 cells were transiently transfected with the siRNAs (50 nM) using INTERFERin (Polyplus).

Western blotting

Samples were collected by direct cell lysis (including pelleted apoptotic cells) in 1x Sample Buffer supplemented with 5% v/v β -mercaptoethanol and heat-denatured at 95°C for 10 minutes. The separated proteins were blotted onto PVDF membranes before antibody incubation in 1% BSA in TBS-Tween20. Antibodies: mouse-anti-GFP (Roche); rabbit-

anti-I κ B α (Cell Signaling); rabbit-anti-Nrf2 (H300, Santa-Cruz); mouse-anti-caspase-8 (Cell Signaling); rabbit-anti-cleaved PARP (Cell Signaling); mouse-anti-Tubulin (Sigma).

Microscopy

Real-time apoptosis induction was determined by monitoring the accumulation of Annexin-V-Alexa633 labeled cells over a 24 hour time period (26). For this, transmission and Alexa633 images of the same area with cells were taken automatically every 30 minutes using a BD Pathway™ 855 bioimager and a 10x Olympus PlanApo lens.

Stabilization of Srxn1-GFP or nuclear oscillation of GFP-p65 was monitored using a Nikon TIE2000 confocal laser microscope (lasers: 488nm and 408nm), equipped with an automated stage and perfect focus system. Prior to imaging at 20x magnification, HepG2 cells were loaded for 45 minutes with 100ng/mL Hoechst₃₃₃₄₂ to visualize the nuclei, upon which the Hoechst-containing medium was washed away to avoid Hoechst phototoxicity (27). Srxn1-GFP cells were imaged every 30 minutes across a 24 hour time span, GFP-p65 cells every 6 minutes for 6 hours.

Image quantification

To quantify the total pixel area occupied by cells or the number of cells per field imaged, transmission images and Hoechst images respectively were analyzed using ImagePro 7.0 (Media Cybernetics). The accumulation of apoptotic cells or the appearance of Srxn1-GFP positive cells was quantified as the total number of pixels above background. The apoptotic pixel total was normalized for the total cell area. The number of adjacent fluorescent Srxn1-GFP pixels above background (with a minimum size of 45 pixels) was multiplied by the average density of those pixels as a measure for the GFP signal-intensity increase and normalized for the amount of nuclei.

To quantify the nuclear translocation of GFP-p65, nuclei (Hoechst) masks are segmented and tracked in ImageJ to define the GFP-p65 nuclear intensity, followed by cytoplasm segmentation. The normalized nuclear / cytoplasmic intensity ratio for each cell is recorded and further analyzed for different oscillation features, also using ImageJ, including the number of translocations, time period of each individual peak, intensity of the peaks, delay between peaks, and nuclear entry and exit rates (Di Z., Herpers B., Fredriksson L., *et al.*, submitted for publication).

Statistics

All experiments are performed at least in triplicate. Error bars indicate Standard Error, unless indicated otherwise. Statistical comparisons were done in a one-way ANOVA. P-value indications: P<0.05 (*); P<0.01 (**); P<0.001 (***)

RESULTS

Drug-induced cell death of human HepG2 cells

To establish a strategy for a mechanism-based evaluation of adverse drug liver toxicities in *in vitro* models we assembled a list of 15 compounds linked to various types of adverse drug liver toxicity (Supporting Table 1). HepG2 cells were chosen as a model system since genetic manipulation allows the integration of fluorescent reporter constructs for live cell imaging approaches. First we incubated cells in presence of Alexa633-labeled AnnexinV and used live cell imaging to determine the concentration-dependent onset of apoptotic cell death. While none of the compounds induced an overwhelming amount of cell death, our sensitive and robust method allowed us to identify a concentration-dependent HepG2 cell apoptosis for AMI, AMAP, APAP, CBZ, CLZ, DCF, KTZ, NFZ, NTF and SN. Little apoptosis was observed for INH, MTX, NPX, OFX and TGZ. For further experiments for each compounds we defined a concentration that is mildly cytotoxic (indicated in Fig. 1 A) to establish the effect on Nrf2 activation, NF- κ B signaling and in relation to co-exposure to the pro-inflammatory cytokine TNF α .

A BAC-Srxn1-GFP HepG2 cell line reports xenobiotic-mediated Nrf2 activation

Rising levels of oxidative stress leads to activation of the antioxidant pathway, controlled by the transcription factor Nrf2. We first monitored the dynamics of Nrf2 stabilization in our HepG2 model. Menadione (20 μ M, MEN), di-ethyl maleate (100 μ M, DEM) and iodoacetamide (10 μ M, IAA) are potent pro-oxidant xenobiotics that time-dependently stabilize Nrf2 in HepG2 cells (Fig. 1 B). Also KTZ and DCF for which phase I and II metabolism has been demonstrated in HepG2 cells (13, 28) caused stabilization of Nrf2. To visualize the Nrf2 activation in real time, we generated HepG2 reporter cells expressing the Nrf2 target gene Sulfiredoxin (Srxn1) coupled to GFP, controlled by its own promoter, by BAC recombineering (25). Under normal conditions, the Srxn1-GFP reporter is not expressed, but exposure to MEN, DEM, IAA, H₂O₂, DCF and KTZ induced a strong time-dependent expression of GFP-Srxn1 (Fig. 1 C) which was easily detected by confocal microscopy live-cell imaging (Fig. 1 D-E). Quantification of the Srxn1-GFP signal shows that activation of the Nrf2 response by the different Nrf2-inducing compounds follows differential activation patterns. All compounds activated the Srxn1-GFP expression within 8 hours. However, while MEN, DEM, IAA and H₂O₂ induce acute Srxn1-GFP expression upon a lag-phase of 4 hours, the hepatotoxicants DCF and KTZ induce a gradual increase of the Nrf2 activity reporter over time (Fig. 1 E), possibly related to reactive metabolite formation. Importantly, the Srxn1-GFP expression in our model is Nrf2-dependent, since transfection with siRNA oligos targeting Nrf2 inhibits the expression of Srxn1-GFP after exposure to MEN, DEM, DCF and KTZ (Fig. 1 F). Moreover, also Keap1 knockdown which caused an expected stabilization of Nrf2, strongly induced Srxn1-GFP levels.

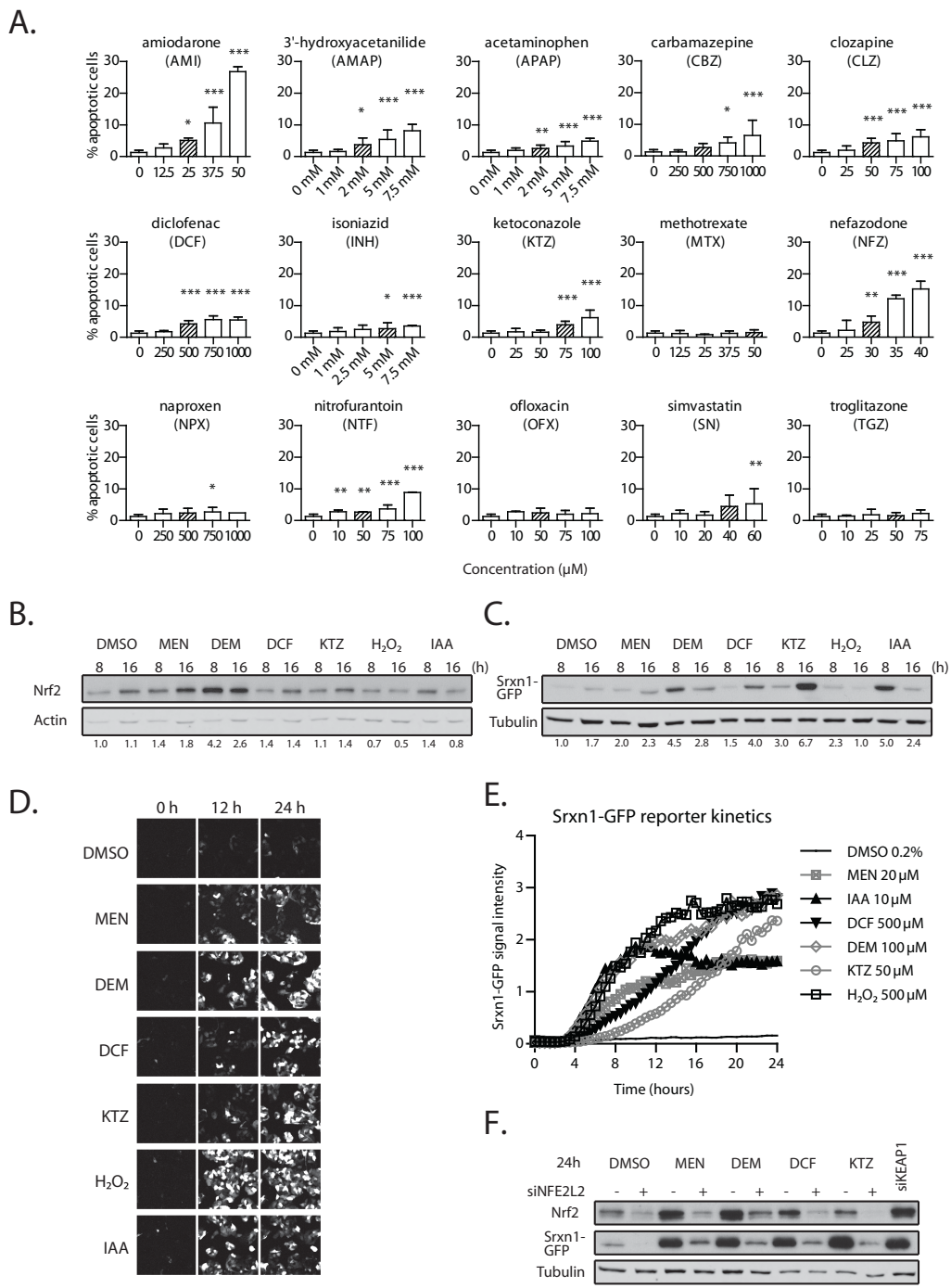


Figure 1. Drug-induced apoptosis and oxidative stress (A) Percentage of apoptotic HepG2 cells at 24 hours after exposure to fifteen different drugs. Concentrations are indicated in μM , except for AMAP, APAP and INH: in mM. "0": 0.2% (v/v) DMSO. Shaded bars: concentration used in subsequent assays. (B) Western blot of Nrf2 expression in HepG2 cells exposed for 8 or 16 hours. (C) Western blot of GFP expression in HepG2 Srnx1-GFP cells. (D) Stills of time-lapse image series of HepG2 Srnx1-GFP cells exposed to Nrf2 inducers. (E) Quantification of the Srnx1-GFP reporter response kinetics. (F) Knockdown of Nrf2 (siNFE2L2) and Keap1 (siKEAP1) in HepG2 Srnx1-GFP cells upon 24h treatment.

DILI compounds activate the Nrf2 stress response independent of TNFR activation

Next, we systematically tested the panel of liver toxicants on the HepG2 Srxn1-GFP reporter cells and monitored the increase of the GFP signal by live-cell imaging (Fig. 2 A-B). We observed that APAP and its regioisomer AMAP potently induce the oxidative stress reporter, as soon as 4 hours after compound exposure. The drugs CBZ, CLZ, DCF, KTZ, NFZ and NTF strongly induced the Srxn1-GFP reporter 8 hours after compound exposure. AMI, MTX and NPX are weak oxidative stress inducers, and Srxn1-GFP induction was observed with delayed kinetics, at 16 hours after compound exposure. The drugs INH, OFX, SN and TGZ did not lead to oxidative stress induction within the 24-hour imaging period in our cell system. These results were confirmed by Western blot (Fig. 2 C-D).

Next, we addressed the question whether TNF α (10 ng/ml) co-exposure increases the rate of Nrf2 stabilization. TNF α has been reported to induce ROS formation, which can be counterbalanced by NF- κ B driven production of anti-oxidant genes (29). However, as an anti-oxidant transcription factor, Nrf2 is potentially involved in this process as well. We observed no significant rise in Nrf2 stabilization or Srxn1-GFP expression when the HepG2 Srxn1-GFP cells were exposed to TNF α alone (Fig. 2 C and D). Since most of our test drugs induced activation of the Nrf2 response 8 hours after drug exposure, we pre-incubated for 8 hours before addition of 10 ng/ml TNF α and assessed the effect of TNF α on the activity of the oxidative stress response 24 hours after the start of the exposure. No significant increase in Nrf2 responses by compound-TNF α combination was observed (Fig. 2 C and D).

Multiparametric analysis of HepG2/GFP-p65 cells to monitor spatio-temporal NF- κ B responses

TNF α promotes liver cell injury under hepatotoxicant treatment conditions. We previously demonstrated that this is related to perturbations of NF- κ B signaling by TNF α (13). To monitor the effect of the hepatotoxicants on the execution of the NF- κ B response, we used a previously established HepG2 cell line expressing GFP-tagged p65/RelA, a subunit of the dimeric transcription factor NF- κ B. This GFP-p65 reporter allows us to follow and quantify the spatio-temporal nuclear translocation of NF- κ B. TNF α promotes phosphorylation and subsequent degradation of the NF- κ B inhibitor I κ B α in an oscillatory manner (Fig. 3 A) which is followed by nuclear translocation of NF- κ B that oscillates in time (Fig. 3 B: top panel). This activity is IKK-dependent, because an 8 hour pre-incubation with 2 μ M BMS-345541, a potent IKK β inhibitor, resulted in inhibition of the NF- κ B oscillation response (Fig. 3 B). Quantification of the nuclear/cytoplasmic ratio of the GFP-p65 NF- κ B reporter construct (based on ~1000 individual cells per condition) revealed that BMS-345541 not only inhibits the NF- κ B response in relation to the number of nuclear translocation events at 0.5 μ M, but also the translocation amplitude of the GFP-p65 signal (Fig. 3 C). Extraction of multiple parameters from the oscillation pattern of all individual cells

within the observed population revealed that the IKK β inhibition caused a concentration-dependent decrease in the number of cells oscillating upon TNF α stimulation, together with an increase in the time of the second nuclear translocation maximum (150 minutes

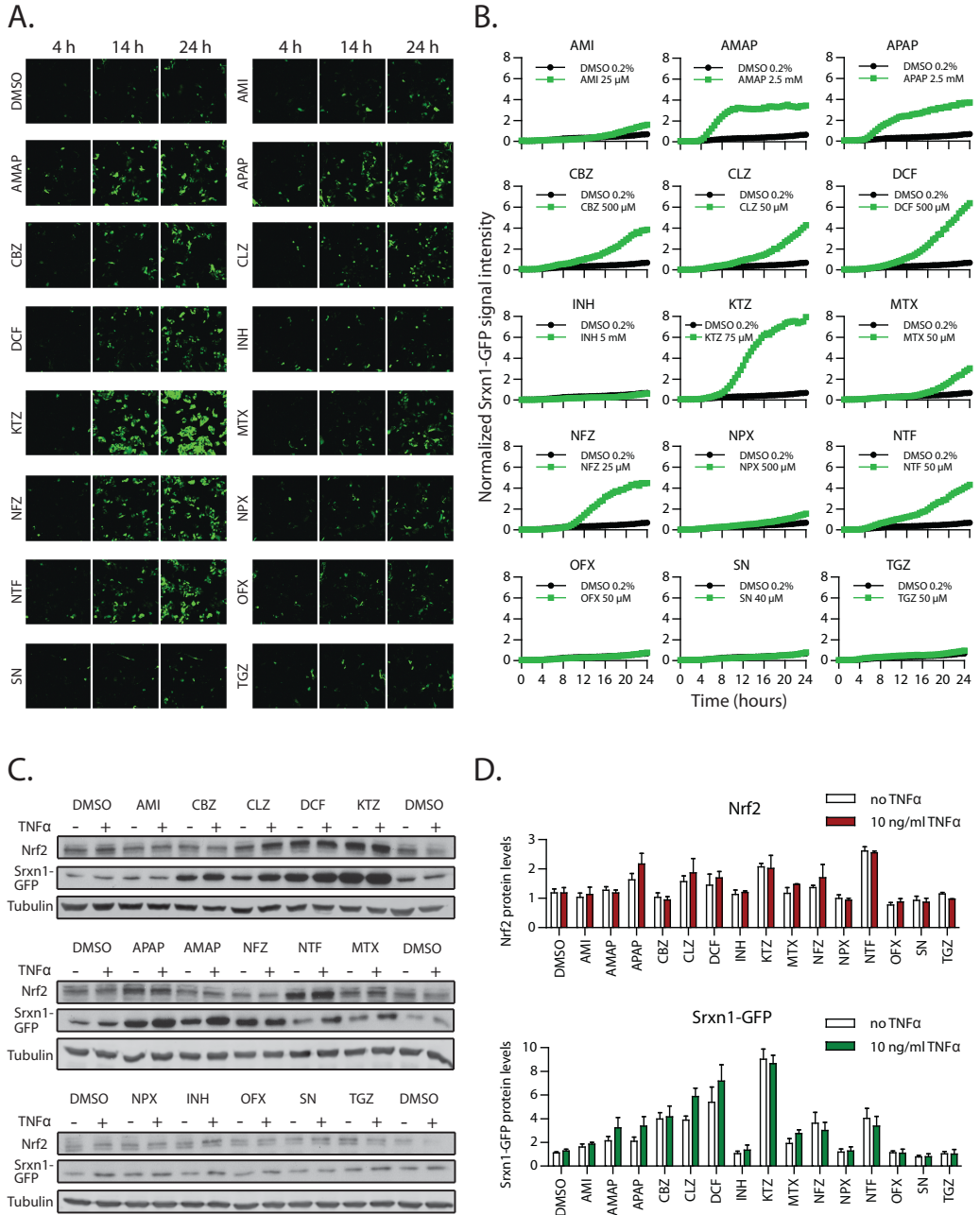


Figure 2. Drug exposure induces dynamically divergent Nrf2 responses. (A) Stills of live-cell imaging on HepG2 Srxn1-GFP cells upon drug exposure (shown are 4, 14 and 24 hours). (B) Quantification of the Srxn1-GFP signal appearing upon drug exposure. (C) Western-blots for Nrf2 and GFP expression after 24 hour drug exposure in HepG2 Srxn1-GFP cells, either with or without co-exposure to 10ng/ml TNF α . (D) Quantification of the Nrf2 and Srxn1-GFP protein levels, 24h after drug +/- TNF α exposure.

in control conditions, 186 minutes at low BMS-345541 concentrations, and 216 minutes at the highest concentration) (Fig. 3 D). These data indicate that this GFP-p65 HepG2 reporter cell line in combination with high content imaging provides thorough insight in the perturbations of the NF- κ B signaling that fit with the biochemistry.

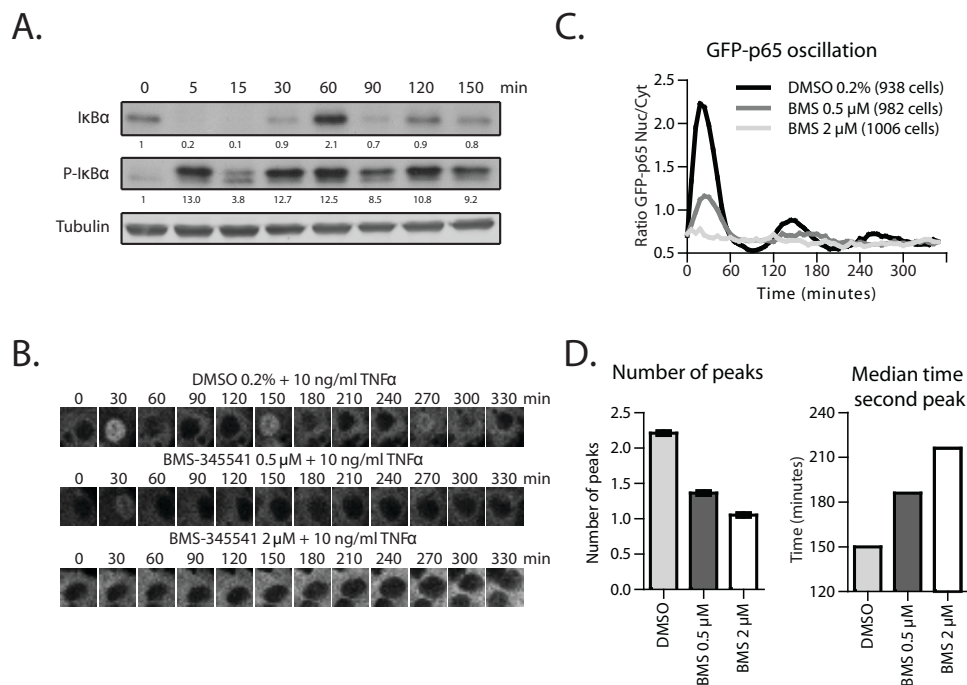


Figure 3. TNF α stimulation induces IKK β -dependent NF- κ B oscillations. (A) 10 ng/ml TNF α stimulation induces IkB α phosphorylation and degradation, followed by IkB α re-synthesis and degradation. (B) HepG2 GFP-p65 (NF- κ B reporter) cells treated for 8 hours with the IKK β -inhibitor BMS-345541 before TNF α exposure show impaired NF- κ B nuclear translocation. (C) Quantification of the nuclear/cytoplasmic GFP-p65 intensity ratio in control (0.2% DMSO) and BMS-345541 treated cells upon TNF α stimulation. (D) Statistical analysis of the HepG2 GFP-p65 cell population under control versus BMS-345541 conditions.

DILI compounds cause a perturbation of NF- κ B signaling

Next we tested the effect of DILI compound treatment on TNF α -induced NF- κ B activation. We selected an 8-hour drug pre-incubation period before the addition of TNF α . As reported previously, DCF delayed the second translocation event (+20 min) (Fig. 4 A). AMI (+20 minutes), CBZ (+20 minutes) and NTF (+20 minutes) delayed the oscillation to a similar extent as DCF. Already at 25 μ M KTZ strongly delayed the oscillation by 37 minutes. NFZ delayed the oscillation by 30 minutes. Pretreatment with CLZ and MTX only weakly perturbed the appearance of the second translocation response with a delay of 10 and 16 min, respectively. Neither AMAP, APAP, INH, OFX, SN nor TGZ significantly influenced the translocation maximum of the second nuclear translocation event.

Detailed cell population-based quantitative analysis of the translocation response

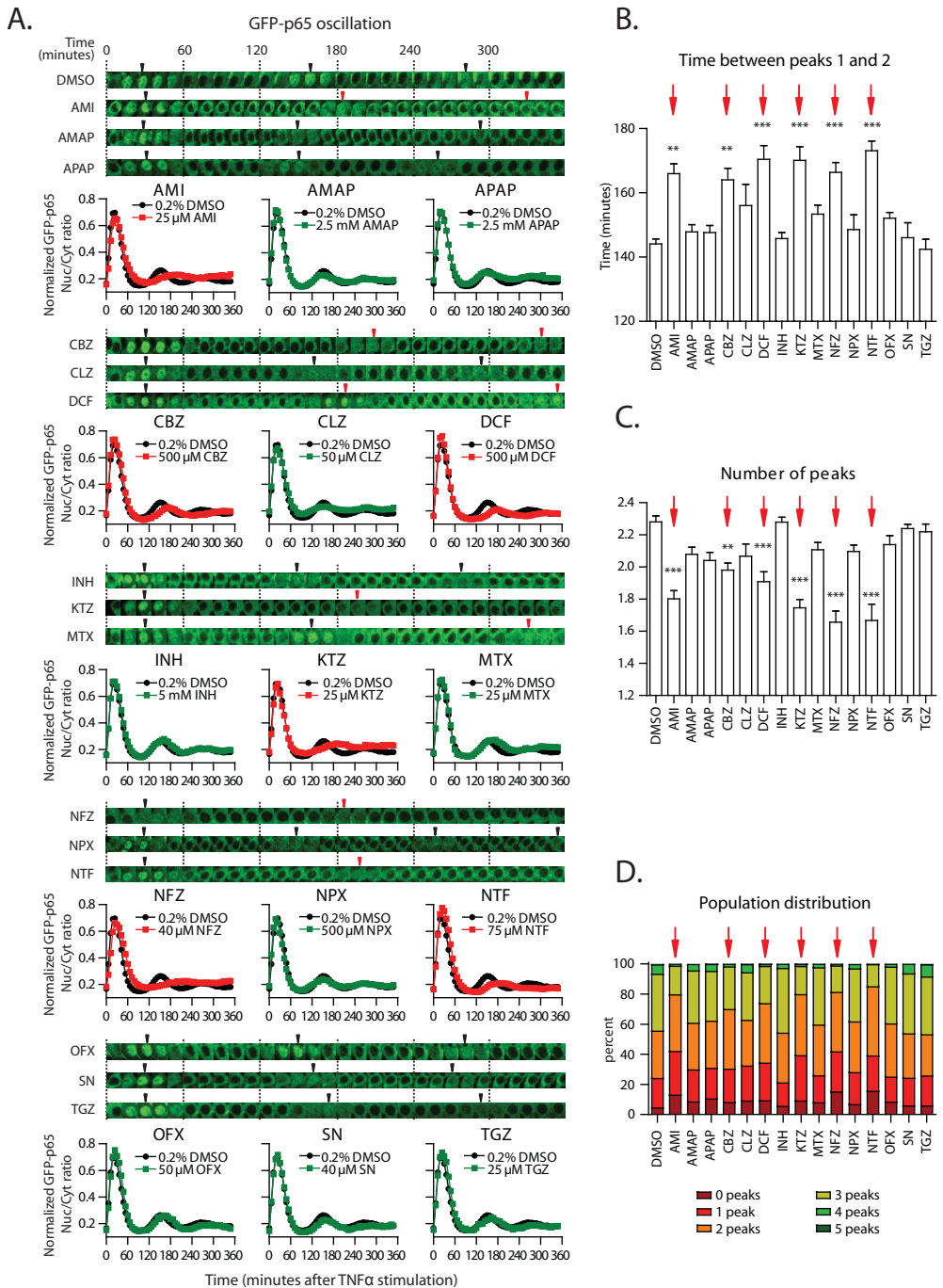
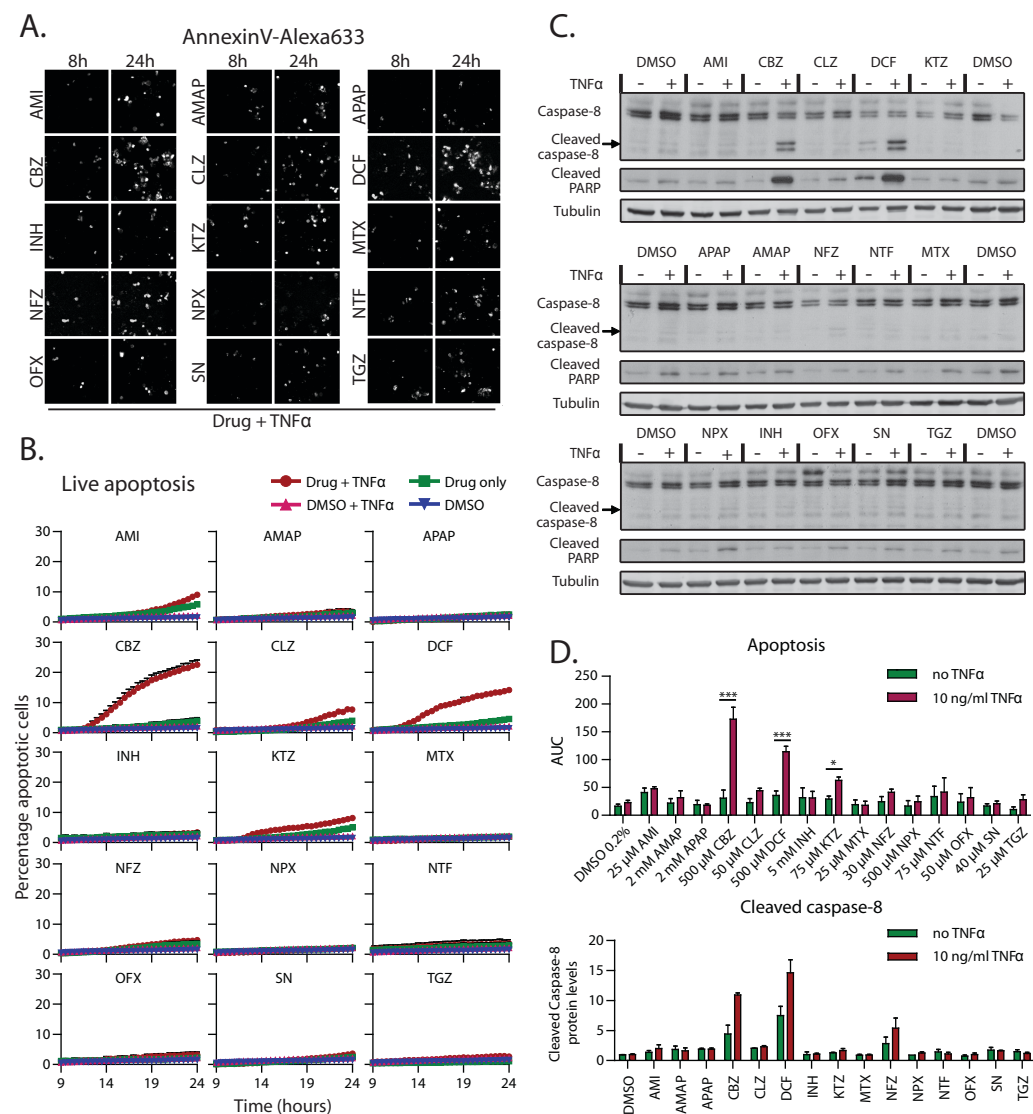


Figure 4. Drug-impaired NF- κ B activation. (A) Time-lapse images of one representative cell showing NF- κ B oscillation upon 10 ng/ml TNF α stimulation after an 8-hour drug pre-incubation period. Arrowheads point at the local nuclear translocation maxima. Quantified average of the GFP-p65 nuclear/cytoplasmic intensity ratio, normalized between 0 and 1 to focus on the appearance of the nuclear translocation maxima (peaks). (B) Analysis of the NF- κ B response: time between peaks 1 and 2. (C) Analysis of the NF- κ B response: assessment of the number of peaks. (D) Distribution of the TNF α -stimulated, drug pre-exposed cell population, classified for showing 0 to 5 peaks within the 6-hour imaging period.

allows extraction of various parameters that describe the NF- κ B oscillation response to TNF α . Indeed, pre-treatment with AMI, CBZ, DCF, KTZ, NFZ or NTF significantly affects the time between the translocation maxima 1 and 2 (Fig. 4 B) and thereby reduces the average number of translocation events within the 6-hour imaging window (Fig. 4 C). Importantly, by evaluating the cell distribution of on average \sim 1000 cells per condition, we identified that AMI, CBZ, DCF, KTZ, NFZ and NTF in general increased the percentage



of cells with only one or two nuclear translocation peaks, and thereby decreased the percentage of cells with three or more NF- κ B nuclear translocation events (Fig. 4 D).

DILI compound and TNF α synergy towards apoptosis

Since TNF α drives a NF- κ B-dependent pro-survival response we anticipated that the inhibitory effect of drug pre-exposure on the NF- κ B response might sensitize HepG2 cells towards apoptosis. To address this we systematically analyzed the compound-TNF α apoptosis synergy upon 8-hour drug pre-treatment followed by TNF α treatment. We monitored the onset of apoptosis within a 24-hour time period by live-cell imaging of AnnexinV-Alexa633 (Fig. 5 A). TNF α clearly enhanced the cell killing for CBZ, DCF and KTZ compared to the drugs alone. The cell killing for the other compounds was low, yet a significant increase in apoptosis under drug/TNF α conditions could be observed for AMI, CLZ and NFZ (Fig. 5 B). To further evaluate the onset of apoptosis, we monitored caspase-8 activation and PARP cleavage as markers of death receptor mediated cell killing. In accordance with the live apoptosis assay, we found a marked increase in cleaved caspase-8 and caspase-cleaved PARP under DCF/TNF α and CBZ/TNF α co-exposure conditions (Fig. 5 C and D).

Integrated analysis of Nrf2, NF- κ B and apoptosis high content live cell imaging assays

Finally we evaluated the relationship between Nrf2 activation, NF- κ B signaling perturbations and compound/TNF α synergy. For all markers we defined the response from absent to very strong and accordingly ranked the compounds based on their synergy response (Table 1). Firstly, the data indicate that there is not a necessary correlation between Nrf2 activation and NF- κ B inhibition, since both AMAP and APAP have a strong Srxn1-GFP induction but hardly affect the NF- κ B response. In this situation also no cytotoxic synergy is observed. Yet for almost all compounds that show some synergy response for apoptosis, a strong Srxn1-GFP induction as well as a delayed NF- κ B nuclear oscillation is observed.

DISCUSSION

Whether a candidate drug in the development phase harbors an increased risk for liver failure remains difficult to predict due to the lack of adequate biomarkers and predictive *in vitro* and *in vivo* models. In this manuscript we propose the integration of three high content quantitative microscopy live cell imaging-based *in vitro* approaches to systematically analyze and classify the effect of drug exposure over time by addressing the biochemical mechanism (oxidative stress-based Nrf2 activation), the immune response mechanism (NF- κ B signaling) and the cell death response (apoptosis).

Drug metabolism can create reactive soft electrophiles which are eradicated by

Table 1. Overview of the test results derived from the Srxn1-GFP assay (Nrf2 response), the GFP-p65 assay (NF- κ B response) and the Annexin-V apoptosis assay (TNF α -enhanced apoptosis).

Drug	Nrf2 response		NF- κ B response		TNF α -enhanced apoptosis			
	Fold increase Srxn1-GFP	Initiation (hours)	delay 2nd peak (minutes)	Oscillations (#)	24h drug only (%)	24h drug + TNF α (%)	Differ ence (%)	Synergy initiation (hours)
CBZ	3.2	10	20	1.98	2.8	21.8	18.9	12
DCF	5.7	10	20	1.91	3.8	13.6	9.8	12
KTZ	7.3	8	37	1.75	4.1	6.7	2.7	12
CLZ	3.6	11	10	2.07	3.3	5.3	2.0	22
NFZ	3.8	10	20	1.66	2.8	4.4	1.6	23
AMI	0.9	19	20	1.8	5.0	7.1	2.1	23
NTF	3.6	8	30	1.67	1.5	1.8	0.3	>24
AMAP	3.0	5	5	2.11	1.3	2.6	1.3	19
APAP	3.0	5	6	2.04	2.1	2.4	0.4	>24
MTX	2.3	17	16	2.11	1.0	1.4	0.5	>24
NPX	0.8	20	0	2.1	1.0	1.9	0.9	>24
TGZ	0.3	>24	0	2.22	0.7	1.8	1.1	19
SN	0.1	>24	3	2.24	1.8	1.8	0	>24
OFX	0.1	>24	6	2.14	1.1	2.1	1.0	24
INH	0.0	>24	0	2.28	1.4	2.4	1.1	24
DMSO	0.0	>24	0	2.28	0.8	1.3	0.5	>24

further phase 2 drug metabolism or scavenged by glutathione (GSH). GSH depletion is sensed by the Nrf2-Keap1 system, which responds by Nrf2-driven increases in GSH production. Alternatively, reactive metabolites may covalently modify free cysteine moieties in Keap1. To monitor activation of the Nrf2-Keap1 as a measure for reactive metabolite formation, we made advantage of a bacterial artificial chromosome-based Sulfiredoxin (Srnx1)-GFP reporter, driven by the endogenous promoter of Srnx1, which is fully dependent on Nrf2. Most DILI compounds showed activation of the Nrf2 response suggesting that reactive metabolites are formed by these compounds. Indeed in an earlier study we demonstrated metabolite formation for DCF (13). We observed for APAP and its regioisomer AMAP a fast Srnx1-GFP induction, similar to the GSH-depleting agents DEM and IAA, suggesting a direct effect for GSH depletion on the Nrf2 induction. Sustained Nrf2 stabilization, indicating persistent Nrf2 activation, was found for CLZ, DCF, KTZ, NFZ and NTF, possibly modifying Keap1 through reactive metabolites, which correlated with Srnx1-GFP induction. No effect was found on the Nrf2 response or the Nrf2 reporter in HepG2 cells for the drugs INH, NPX, OFX, SN and TGZ. This effect might be due to the low expression of cytochrome P450 enzymes in HepG2 cells, compared to primary hepatocytes (30), the FBS concentration (10 %) used (31), the duration of the experiments, or the chosen concentration (32). Since the redox-cycling agent MEN as well as H₂O₂ also activated Srnx1-GFP expression, at this moment we cannot entirely exclude that the observed effect for the DILI compounds is (partly) related to secondary oxidative stress, possibly derived from mitochondrial toxicity. Further research is required to identify the exact mechanism of Nrf2 activation for the different DILI compounds.

Stimulation of HepG2 cells with TNF α activates the IKK complex, which is essential for the activation of the downstream NF- κ B response. We showed that a strong

drug-induced Nrf2 activation for the drugs AMI, CBZ, DCF, KTZ, NFZ and NTF closely correlated with a delay in the timing of the nuclear translocation peaks of NF- κ B. Yet, while APAP also caused Nrf2 activation, this was not associated to a delay in the NF- κ B oscillation. We speculate that the crosstalk between the Nrf2 and NF- κ B signaling is apparently not mediated through Nrf2 activation *per se*. Alternatively, the reactive metabolites derived from AMI, CBZ, DCF, KTZ, NFZ and NTF likely affect a broader set of intracellular sensors and, thereby, affect alternative signaling pathways, including Nrf2 and NF- κ B signaling. APAP-derived metabolites presumably only affect the Nrf2 pathway. This difference in response is likely related to different reactivity of the metabolites and/or the intracellular sites where they are generated. More work is required to identify the levels of metabolite formation and their cellular targets for the DILI compounds we used. Moreover, it will be highly relevant to determine which compounds directly affect the Nrf2 activation through covalent modification of Keap1.

In case of combined Nrf2 activation and NF- κ B suppression an increased risk for drug-cytokine cytotoxic synergy may be present. The working model for immune-related DILI suggests the imbalance between pro-inflammatory cytokine and anti-inflammatory cytokine signaling as a critical initiator of hepatocyte cell killing (11, 12). We observed the strongest TNF α -enhanced drug-induced apoptosis for CBZ, DCF and KTZ, and more weakly for NFZ, AMI and CLZ. These six drugs activate both the Srxn1-GFP reporter and induce a delay in the NF- κ B response, albeit that the effect of CLZ at 50 μ M on NF- κ B oscillation was not significant (10-minute delay), yet at 75 μ M the effect became significant (20 minutes). This suggests that monitoring the ability of drugs to activate the Nrf2 response and determining the drug effect on NF- κ B oscillations can be indicative for sensitization towards pro-inflammatory cytokines during drug exposure, as a sign for increased risk of DILI potential. We are currently investigating the underlying molecular mechanisms through RNA-interference-based functional genomics strategies and our findings indicate a critical role for the translational control component EIF4A1 in close relationship to the expression of the pro-apoptotic unfolded protein response gene CHOP/DDIT3 (Fredriksson *et al.*, submitted).

In conclusion, we have established a systems microscopy approach using high content confocal microscopy live-cell imaging in combination with automated multiparametric quantitative image analysis to monitor in parallel the kinetics of apoptosis, Nrf2 activation and the NF- κ B oscillatory response. Our systems microscopy assays are more quantitative, robust, reliable and more informative than standard protein quantification, because single cells within a large population can be monitored across time. Furthermore, the approach can be multiplexed: the Srxn1-GFP reporter can be combined with Annexin-V or propidium-iodide to monitor oxidative stress simultaneously with apoptosis or necrosis induction, respectively. We are aware that our current strategy does not positively identify all DILI compounds. Given the diversity of molecular mechanisms for DILI, we would not expect this. Although the monolayer cultures of our HepG2 reporter cells provide greater speed and accuracy, we understand that their limited differentiation status is posing some limitations. Currently we are establishing 3D

spheroid cultures of HepG2 cells to increase their differentiation status and increase the levels of phase 1 and 2 metabolism. Preliminary results using 3D HepG2-Srxn1-GFP cells for high content imaging shows induction of Srxn1-GFP expression by TGZ. While we have limited ourselves to Nrf2 and NF- κ B signaling in this study, further development of additional cell injury reporters (e.g. mitochondrial function, ER-stress and DNA damage) is ongoing. We anticipate that the application of such models in combination with DILI compound, cytokine and siRNA screening will greatly contribute to the mechanistic understanding of adverse drug reactions.

3

ACKNOWLEDGEMENTS

The authors like to thank the TI-Pharma consortium for critically reading the manuscript and members of the division of Toxicology for help and scientific discussions.

FUNDING

This work was funded by the TI-Pharma project D3-201 and IMI-MIP-DILI project to BvdW and the NCI Horizon project 9351008 to BH.

REFERENCES

1. Park BK, Laverty H, Srivastava A, Antoine DJ, Naisbitt D, Williams DP. Drug bioactivation and protein adduct formation in the pathogenesis of drug-induced toxicity. *Chem Biol Interact* 2010.
2. Srivastava A, Maggs JL, Antoine DJ, Williams DP, Smith DA, Park BK. Role of reactive metabolites in drug-induced hepatotoxicity. *Handb Exp Pharmacol* 2010;165-194.
3. Jones DP, Lemasters JJ, Han D, Boelsterli UA, Kaplowitz N. Mechanisms of pathogenesis in drug hepatotoxicity putting the stress on mitochondria. *Mol Interv* 2010;10:98-111.
4. Uetrecht J. Immunoallergic drug-induced liver injury in humans. *Semin Liver Dis* 2009;29:383-392.
5. Li J, Uetrecht JP. The danger hypothesis applied to idiosyncratic drug reactions. *Handb Exp Pharmacol* 2010;493-509.
6. Naisbitt DJ, Williams DP, Pirmohamed M, Kitteringham NR, Park BK. Reactive metabolites and their role in drug reactions. *Curr Opin Allergy Clin Immunol* 2001;1:317-325.
7. Pichler WJ, Beeler A, Keller M, Lerch M, Posadas S, Schmid D, Spanou Z, et al. Pharmacological interaction of drugs with immune receptors: the p-i concept. *Allergol Int* 2006;55:17-25.
8. Pirmohamed M, Naisbitt DJ, Gordon F, Park BK. The danger hypothesis--potential role in idiosyncratic drug reactions. *Toxicology* 2002;181-182:55-63.
9. Lucas M, Stuart LM, Savill J, Lacy-Hulbert A. Apoptotic cells and innate immune stimuli combine to regulate macrophage cytokine secretion. *J Immunol* 2003;171:2610-2615.
10. Deng X, Stachlewitz RF, Liguori MJ, Blomme EA, Waring JF, Luyendyk JP, Maddox JF, et al. Modest inflammation enhances diclofenac hepatotoxicity in rats: role of neutrophils and bacterial translocation. *J Pharmacol Exp Ther* 2006;319:1191-1199.
11. Shaw PJ, Ganey PE, Roth RA. Idiosyncratic drug-induced liver injury and the role of inflammatory stress with an emphasis on an animal model of trovafloxacin hepatotoxicity. *Toxicol Sci* 2010;118:7-18.
12. Cosgrove BD, King BM, Hasan MA, Alexopoulos LG, Farazi PA, Hendriks BS, Griffith LG, et al. Synergistic drug-cytokine induction of hepatocellular death as an in vitro approach for the study of inflammation-associated idiosyncratic drug hepatotoxicity. *Toxicol Appl Pharmacol* 2009;237:317-330.
13. Fredriksson L, Herpers B, Benedetti G, Matadin Q, Puigvert JC, de Bont H, Dragovic S, et al. Diclofenac inhibits tumor necrosis factor-alpha-induced nuclear factor-kappaB activation causing synergistic hepatocyte apoptosis. *Hepatology* 2011;53:2027-2041.
14. Kaspar JW, Niture SK, Jaiswal AK. Nrf2:INrf2 (Keap1) signaling in oxidative stress. *Free Radic Biol Med* 2009;47:1304-1309.
15. Copple IM, Goldring CE, Kitteringham NR, Park BK. The Nrf2-Keap1 defence pathway: role in protection against drug-induced toxicity. *Toxicology* 2008;246:24-33.
16. Zhang DD, Hannink M. Distinct cysteine residues in Keap1 are required for Keap1-dependent ubiquitination of Nrf2 and for stabilization of Nrf2 by chemopreventive agents and oxidative stress. *Mol Cell Biol* 2003;23:8137-8151.
17. McMahon M, Lamont DJ, Beattie KA, Hayes JD. Keap1 perceives stress via three sensors for the endogenous signaling molecules nitric oxide, zinc, and alkenals. *Proceedings of the National Academy of Sciences of the United States of America* 2010;107:18838-18843.
18. Copple IM, Goldring CE, Kitteringham NR, Park BK. The keap1-Nrf2 cellular defense pathway: mechanisms of regulation and role in protection against drug-induced toxicity. *Handb Exp Pharmacol* 2010:233-266.
19. Chan K, Han XD, Kan YW. An important function of Nrf2 in combating oxidative stress: detoxification of acetaminophen. *Proc Natl Acad Sci U S A* 2001;98:4611-4616.
20. Copple IM, Goldring CE, Jenkins RE, Chia AJ, Randle LE, Hayes JD, Kitteringham NR, et al. The hepatotoxic metabolite of acetaminophen directly activates the Keap1-Nrf2 cell defense system. *Hepatology* 2008;48:1292-1301.
21. Liguori MJ, Ditewig AC, Maddox JF, Luyendyk JP, Lehman-McKeeman LD, Nelson DM, Bhaskaran VM, et al. Comparison of TNFalpha to Lipopolysaccharide as an Inflammagen to Characterize the Idiosyncratic Hepatotoxicity Potential of Drugs: Trovafloxacin as an Example. *International journal of molecular sciences* 2010;11:4697-4714.
22. Wullaert A, Heyninck K, Beyaert R. Mechanisms of crosstalk between TNF-induced NF-kappaB and JNK activation in hepatocytes. *Biochem Pharmacol* 2006;72:1090-1101.
23. Ashall L, Horton CA, Nelson DE, Paszek P, Harper CV, Sillitoe K, Ryan S, et al. Pulsatile stimulation determines timing and specificity of NF-kappaB-dependent transcription. *Science* 2009;324:242-246.
24. Enesa K, Ito K, Luong le A, Thorbjornsen I, Phua C, To Y, Dean J, et al. Hydrogen peroxide prolongs nuclear localization of NF-kappaB in activated cells by suppressing negative regulatory mechanisms. *J Biol Chem* 2008;283:18582-18590.
25. Hendriks G, Atallah M, Morolli B, Calleja F, Ras-Verloop N, Huijskens I, Raamsman M, et al. The ToxTracker assay: novel GFP reporter systems that provide mechanistic insight into the genotoxic

- properties of chemicals. *Toxicol Sci* 2012;125:285-298.
26. Puigvert JC, de Bont H, van de Water B, Danen EH. High-throughput live cell imaging of apoptosis. *Curr Protoc Cell Biol* 2010;Chapter 18:Unit 18 10 11-13.
 27. Purschke M, Rubio N, Held KD, Redmond RW. Phototoxicity of Hoechst 33342 in time-lapse fluorescence microscopy. *Photochem Photobiol Sci* 2010;9:1634-1639.
 28. Gerets HH, Tilmant K, Gerin B, Chanteux H, Depelchin BO, Dhalluin S, Atienzar FA. Characterization of primary human hepatocytes, HepG2 cells, and HepaRG cells at the mRNA level and CYP activity in response to inducers and their predictivity for the detection of human hepatotoxins. *Cell biology and toxicology* 2012;28:69-87.
 29. Trachootham D, Alexandre J, Huang P. Targeting cancer cells by ROS-mediated mechanisms: a radical therapeutic approach? *Nature reviews. Drug discovery* 2009;8:579-591.
 30. Westerink WM, Schoonen WG. Cytochrome P450 enzyme levels in HepG2 cells and cryopreserved primary human hepatocytes and their induction in HepG2 cells. *Toxicol In Vitro* 2007;21:1581-1591.
 31. Yamamoto Y, Nakajima M, Yamazaki H, Yokoi T. Cytotoxicity and apoptosis produced by troglitazone in human hepatoma cells. *Life Sci* 2001;70:471-482.
 32. Nicod L, Viollon C, Regnier A, Jacqueson A, Richert L. Rifampicin and isoniazid increase acetaminophen and isoniazid cytotoxicity in human HepG2 hepatoma cells. *Hum Exp Toxicol* 1997;16:28-34.

SUPPORTING DATA

Supporting Table 1. Drugs used in this study and their reported adverse effects on the liver

Drug name	Abbreviation	Function	Metabolizing enzymes	Adverse drug reactions in the liver	References
amiodarone	AMI	antiarrhythmic agent	CYP3A4; 1A2	ALT/AST elevations; cirrhosis; jaundice; hepatomegaly; hepatitis; phospholipidosis; steatohepatitis; cholestasis	(1, 2)
3-hydroxyacetanilide	AMAP	regioisomer of paracetamol	CYP2E1	Does not cause liver failure in mice	(3, 4)
paracetamol / acetaminophen	APAP	analgesic and antipyretic	CYP2E1; 1A2; 2D6; 3A4	DRESS syndrome; acute liver failure; necrosis	(5-7)
carbamazepine	CBZ	antiepileptic drug	CYP3A4; 2C9; induces CYP3A4	SJS/TEN (Stevens-Johnson syndrome / toxic epidermal necrolysis); chronic hepatitis	(8-11)
clozapine	CLZ	antipsychotic drug	CYP3A4; 1A2; 2D6	ALT/AST elevations; hepatitis; jaundice; necrosis	(12-16)
diclofenac	DCF	NSAID	CYP3A4; 2C9 ; 2C8; UGT2B7	SJS; acute hepatitis; necrosis; autoimmune chronic liver injury	(17-19)
isoniazid	INH	anti-tuberculosis drug	CYP2E1; inhibits CYP2C9 and 3A4	ALT/AST elevation; acute hepatitis; chronic hepatitis; necrosis	(20-22)
ketoconazole	KTZ	antifungal antibiotic	CYP3A4; inhibits CYP3A4 and UGT2B7	acute hepatitis; cholestasis; necrosis	(23-25)
methotrexate	MTX	chemotherapeutic agent	aldehyde oxidase; CYP2E1	ALT/AST elevations; fibrosis; cirrhosis; chronic hepatitis; NASH	(26, 27)
nefazodone	NFZ	antidepressant	CYP3A4; inhibits CYP3A4	liver failure; jaundice; hepatitis; hepatocellular necrosis	(28, 29)
naproxen	NPX	NSAID	CYP2C9	ALT/AST elevations; cholestasis; acute hepatitis	(30)
nitrofurantoin	NTF	antibiotic against urinary tract infections	CYP1A	autoimmune hepatitis; chronic active hepatitis; necrosis	(31, 32)
ofloxacin	OFX	antibiotic	CYP1A2; 2C19	SJS/TEN; hepatocellular necrosis; jaundice; hepatitis	(33)
simvastatin	SN	statin	CYP3A4	ALT/AST elevations; jaundice; hepatitis	(34, 35)
troglitazone	TGZ	antidiabetic	CYP1A1; 2C8; 2C19; 3A4	fulminant hepatitis; ALF	(36, 37)

SUPPORTING REFERENCES

1. Lu J, Jones AD, Harkema JR, Roth RA, Ganey PE. Amiodarone exposure during modest inflammation induces idiosyncrasy-like liver injury in rats: role of tumor necrosis factor- α . *Toxicol Sci* 2012;125:126-133.
2. Pollak PT, Shafer SL. Use of population modeling to define rational monitoring of amiodarone hepatic effects. *Clin Pharmacol Ther* 2004;75:342-351.
3. Stamper BD, Bammler TK, Beyer RP, Farin FM, Nelson SD. Differential regulation of mitogen-activated protein kinase pathways by acetaminophen and its nonhepatotoxic regioisomer 3'-hydroxyacetanilide in TAMH cells. *Toxicol Sci* 2010;116:164-173.
4. Halmes NC, Samokyszyn VM, Hinton TW, Hinson JA, Pumford NR. The acetaminophen regioisomer 3'-hydroxyacetanilide inhibits and covalently binds to cytochrome P450 2E1. *Toxicol Lett* 1998;94:65-71.
5. Jaeschke H, Williams CD, Ramachandran A, Bajt ML. Acetaminophen hepatotoxicity and repair: the role of sterile inflammation and innate immunity. *Liver Int* 2012;32:8-20.
6. Manyike PT, Kharasch ED, Kalthorn TF, Slattery JT. Contribution of CYP2E1 and CYP3A to acetaminophen reactive metabolite formation. *Clin Pharmacol Ther* 2000;67:275-282.
7. Pirmohamed M, Madden S, Park BK. Idiosyncratic drug reactions. *Metabolic bioactivation as a pathogenic mechanism. Clin Pharmacokinet* 1996;31:215-230.
8. Daly AK. Using genome-wide association studies to identify genes important in serious adverse drug reactions. *Annu Rev Pharmacol Toxicol* 2012;52:21-35.
9. Phillips EJ, Mallal SA. HLA-B*1502 screening and toxic effects of carbamazepine. *N Engl J Med* 2011;365:672; author reply 673.
10. Bjornsson E. Hepatotoxicity associated with antiepileptic drugs. *Acta Neurol Scand* 2008;118:281-290.
11. Syn WK, Naisbitt DJ, Holt AP, Pirmohamed M, Mutimer DJ. Carbamazepine-induced acute liver failure as part of the DRESS syndrome. *Int J Clin Pract* 2005;59:988-991.
12. McKnight C, Guirgis H, Votolato N. Clozapine rechallenge after excluding the high-risk clozapine-induced agranulocytosis genotype of HLA-DQB1 6672G>C. *Am J Psychiatry* 2011;168:1120.
13. Dragovic S, Boerma JS, van Bergen L, Vermeulen NP, Commandeur JN. Role of human glutathione S-transferases in the inactivation of reactive metabolites of clozapine. *Chem Res Toxicol* 2010;23:1467-1476.
14. Damsten MC, van Vugt-Lussenburg BM, Zeldenthuis T, de Vlieger JS, Commandeur JN, Vermeulen NP. Application of drug metabolising mutants of cytochrome P450 BM3 (CYP102A1) as biocatalysts for the generation of reactive metabolites. *Chem Biol Interact* 2008;171:96-107.
15. Valevski A, Klein T, Gazit E, Meged S, Stein D, Elizur A, et al. HLA-B38 and clozapine-induced agranulocytosis in Israeli Jewish schizophrenic patients. *Eur J Immunogenet* 1998;25:11-13.
16. Hummer M, Kurz M, Kurtzthaler I, Oberbauer H, Miller C, Fleischhacker WW. Hepatotoxicity of clozapine. *J Clin Psychopharmacol* 1997;17:314-317.
17. Fredriksson L, Herpers B, Benedetti G, Matadin Q, Puigvert JC, de Bont H, et al. Diclofenac inhibits tumor necrosis factor- α -induced nuclear factor- κ B activation causing synergistic hepatocyte apoptosis. *Hepatology* 2011;53:2027-2041.
18. Deng X, Luyendyk JP, Ganey PE, Roth RA. Inflammatory stress and idiosyncratic hepatotoxicity: hints from animal models. *Pharmacol Rev* 2009;61:262-282.
19. Boelsterli UA. Diclofenac-induced liver injury: a paradigm of idiosyncratic drug toxicity. *Toxicol Appl Pharmacol* 2003;192:307-322.
20. Daly AK, Day CP. Genetic association studies in drug-induced liver injury. *Drug Metab Rev* 2012;44:116-126.
21. Srivastava A, Maggs JL, Antoine DJ, Williams DP, Smith DA, Park BK. Role of reactive metabolites in drug-induced hepatotoxicity. *Handb Exp Pharmacol* 2010:165-194.
22. Zand R, Nelson SD, Slattery JT, Thummel KE, Kalthorn TF, Adams SP, et al. Inhibition and induction of cytochrome P4502E1-catalyzed oxidation by isoniazid in humans. *Clin Pharmacol Ther* 1993;54:142-149.
23. Lin CL, Hu JT, Yang SS, Shin CY, Huang SH. Unexpected emergence of acute hepatic injury in patients treated repeatedly with ketoconazole. *J Clin Gastroenterol* 2008;42:432-433.
24. Kim TH, Kim BH, Kim YW, Yang DM, Han YS, Dong SH, et al. Liver cirrhosis developed after ketoconazole-induced acute hepatic injury. *J Gastroenterol Hepatol* 2003;18:1426-1429.
25. Bernuau J, Durand F, Pessayre D. Ketoconazole-induced hepatotoxicity. *Hepatology* 1997;26:802.
26. Aithal GP. Hepatotoxicity related to antirheumatic drugs. *Nat Rev Rheumatol* 2011;7:139-150.
27. West SG. Methotrexate hepatotoxicity. *Rheum Dis Clin North Am* 1997;23:883-915.
28. Xu JJ, Henstock PV, Dunn MC, Smith AR, Chabot JR, de Graaf D. Cellular imaging predictions of clinical drug-induced liver injury. *Toxicol Sci* 2008;105:97-105.
29. Stewart DE. Hepatic adverse reactions associated with nefazodone. *Can J Psychiatry* 2002;47:375-377.

30. Ali S, Pimentel JD, Ma C. Naproxen-induced liver injury. *Hepatobiliary Pancreat Dis Int* 2011;10:552-556.
31. Czaja AJ. Drug-induced autoimmune-like hepatitis. *Dig Dis Sci* 2011;56:958-976.
32. Boelsterli UA, Ho HK, Zhou S, Leow KY. Bioactivation and hepatotoxicity of nitroaromatic drugs. *Curr Drug Metab* 2006;7:715-727.
33. Blum A. Ofloxacin-induced acute severe hepatitis. *South Med J* 1991;84:1158.
34. Bjornsson E, Jacobsen EI, Kalaitzakis E. Hepatotoxicity associated with statins: reports of idiosyncratic liver injury post-marketing. *J Hepatol* 2012;56:374-380.
35. Law M, Rudnicka AR. Statin safety: a systematic review. *Am J Cardiol* 2006;97:52C-60C.
36. Jaeschke H. Troglitazone hepatotoxicity: are we getting closer to understanding idiosyncratic liver injury? *Toxicol Sci* 2007;97:1-3.
37. Kaplowitz N. Idiosyncratic drug hepatotoxicity. *Nat Rev Drug Discov* 2005;4:489-499.

